DP(NASA)-1210
Special Distribution

EFFECT OF HYDROGEN GAS ON METALS AT -30 TO +100°C

Progress Report: July 1, 1968 - June 30, 1969

by

J. A. Donovan, Principal Investigator
R. G. Derrick
M. L. Holzworth

Approved by

R. T. Huntoon, Research Manager
Nuclear Materials Division

November 1969

Prepared for

National Aeronautics and Space Administration
Work Performed Under NASA Purchase Order No. W-12697,
Issued to the United States Atomic Energy Commission

E. I. du Pont de Nemours & Company
Savannah River Laboratory
Aiken, South Carolina

Contract AT(07-2)-1 with the
United States Atomic Energy Commission

ABSTRACT

This is the first report of a NASA-sponsored study at Savannah River Laboratory on the effect of hydrogen gas on metals at -30 to +100°C. During this first year of study experimental techniques were developed for determining the solubility, diffusivity, and permeation of hydrogen in metals. Tritium was used in these studies to increase the sensitivity of the determinations. The initial results on the solubility of tritium in nickel in the range 71 to 227°C agreed with data extrapolated from higher temperatures; tritium solubility in iron in the same temperature range was a factor of ten to several hundred higher than extrapolated values. Measured tritium diffusivities in nickel also agreed with literature values, but values for the diffusivity of tritium in iron were in the lower range of the broad band of published values. These initial data also indicate that cold work increases the solubility of tritium in both iron and nickel. Additionally, the rates of hydrogen permeation through T-1 steel and high purity iron were measured.

CONTENTS

	Page
List of Figures	4
List of Tables	5
Introduction	7
Summary	8
Discussion	9
Materials	9
Solubility Measurements	9
Diffusivity Measurements	14
Permeation Measurements	22
Electron Microscopy	29
Program	29
References	29
Appendix	31

LIST OF FIGURES

Figure		Page
1	Exposure Container for Solubility Specimens	10
2	Tritium Solubility in Iron - Average Values for all Specimens	10
3	Effect of Specimen Condition and Temperature on Tritium Solubility in Iron	12
4	Tritium Solubility in Nickel - Average Values for all Specimens	13
5	Effect of Specimen Condition and Temperature on Tritium Solubility in Nickel	14
6	Chamber Used to Contain Tritiated Specimens for Outgassing Rate Measurements	17
7	Tritium Release Rate from Nickel as a Function of Time at 125°C	17
8	Tritium Release Rate from Nickel as a Function of Time	18
9	Temperature Dependence of Tritium Diffusivity in Nickel	18
10	Tritium Release Rate from Iron as a Function of Time	20
11	Temperature Dependence of Tritium Diffusivity in Iron	20
12	Representative Data for Diffusivity of Hydrogen in Iron	21
13	Characteristic Permeation Curve Used for Time-Lag Analysis	22
14	Schematic Representation of Permeation System	24
15	Permeation of Hydrogen Through T-1 Steel	24
16	Temperature Dependence of Hydrogen Permeability in T-1 Steel	26
17	Permeation of Hydrogen Through 92% Cold-Worked Iron	28
18	Permeation of Hydrogen Through Annealed Iron	28

LIST OF TABLES

Table		Page
I	Solubility Specimens	11
II	Solubility of Tritium in High Purity Iron and Nickel	12
III	Diffusivity of Tritium in Nickel	19
IV	Representative Diffusivities of Hydrogen in Nickel	19
V	Diffusivity of Tritium in Iron	21
VI	Permeability and Diffusivity of Hydrogen in T-1 Steel	25
VII	Permeability and Diffusivity of Hydrogen in High Purity Iron	27

INTRODUCTION

The Savannah River Laboratory is engaged in a program of NASA-sponsored research to develop fundamental knowledge about the mechanism of hydrogen damage to metals in the temperature range -30 to +100°C. This research is of interest to NASA because of recent failures of gaseous hydrogen storage containers.[1-3] The solubility, diffusivity, and permeation of hydrogen in iron and nickel are being emphasized because of their basic importance to the understanding of hydrogen damage and because of the sparsity of information on these metals at low temperatures. The experimental techniques necessary for this program have been developed and preliminary data have been obtained.

One objective of the program is to determine the relation of the microstructure of the metal to hydrogen solubility, diffusivity, and permeability. To achieve this goal, the effects of specimen deformation and grain size are being determined. Electron microscopy will be used to characterize the details of the specimen microstructure. The program will take advantage of the radioactive properties of tritium that provide sufficient sensitivity at low tritium concentrations to obtain meaningful data at near-ambient temperatures.

This is the first annual report to be issued in this program.

SUMMARY

The following experimental techniques for determining solubility, diffusivity, and permeation of hydrogen in metals were developed during the first year of study.

1. Tritium concentration profiles are obtained by exposing specimens to tritium gas at known pressures, and subsequently determining the tritium concentration by liquid scintillation counting of acid solutions used to dissolve layers of predetermined thickness from the specimens. Such concentration gradients can be analyzed to obtain both solubility and diffusivity data.

2. Diffusivity values are also obtained by analysis of isothermal outgassing rates from tritium-exposed specimens.

3. Permeation rates are obtained from pressure-volume measurements in a system which has sufficient sensitivity to be used at near-ambient temperatures. The planned conversion of this system to one in which the permeation rate is measured from the radioactive decay of tritium will increase the sensitivity of the technique.

The following preliminary information was obtained using the above techniques:

1. The solubility of tritium in nickel agreed with values obtained by extrapolation of published high temperature data.

2. The solubility of tritium in iron was significantly higher than predicted from extrapolated high temperature data.

3. Evidence was obtained that cold work increases the solubility of tritium in both iron and nickel.

4. The diffusivity of tritium in nickel, determined from outgassing rate measurements, agreed with published data.

5. The diffusivity of tritium in iron at temperatures below 200°C was at the low end of the broad band of published values.

6. The permeation of hydrogen through T-1 steel was slightly lower than the values established by Gonzalez[4] from a critical examination of the literature.

7. Hydrogen diffusivity, determined by the time-lag analysis of permeation data, was lower by a factor of 10-100 on the initial run than on subsequent runs for the same specimens.

DISCUSSION

MATERIALS

The materials studied in this program are of two classes: high purity metals which provide fundamental data, and engineering alloys which are used in commercial pressure vessels. Major emphasis was on the high purity metals, although some permeation experiments were made on T-1 steel and several diffusivity measurements were made on commercially pure nickel and "Armco"* iron.

The chemical analyses of the various metals are listed in the Appendix.

SOLUBILITY MEASUREMENTS

The solubility of tritium in high purity iron (99.99%) and in nickel (99.995%) was determined for the range 71 to 227°C. Polycrystalline specimens (both cold worked and annealed, Table I), were wafers approximately 0.100 inch thick, cut from 3/8-inch-diameter rods by spark-discharge machining. The as-machined specimens were degreased; the surfaces were then lightly polished on 320-grit paper and rinsed in "Freon"** before loading in flanged, 304L stainless steel containers (Fig. 1). After loading, the containers were sealed, evacuated to 10^{-5} torr, and leak checked to ensure a leak rate of $<10^{-6}$ cc/sec. The leaktight containers were backfilled with 83 mole % tritium to one atmosphere pressure, valved shut, and exposed at the desired temperatures. All data were corrected for the increase in exposure pressure due to thermal expansion of the gas.

After predetermined exposure times, the containers were removed from the furnaces and water quenched to room temperature. The tritium concentration was determined by liquid scintillation analysis of an acid solution in which all or part of the specimen was dissolved. Incremental analyses on randomly chosen specimens verified that the wafers were saturated and that the tritium concentration was constant throughout a specimen. The lowest tritium concentration detected by this technique was 10^{-7} cc T/cc metal. The calculated solubilities are given in Table II.

* Trademark of Armco Steel Co.

** "Freon" and combinations of "Freon-" or "F-" with numerals are Du Pont's registered trademarks for its fluorinated hydrocarbons.

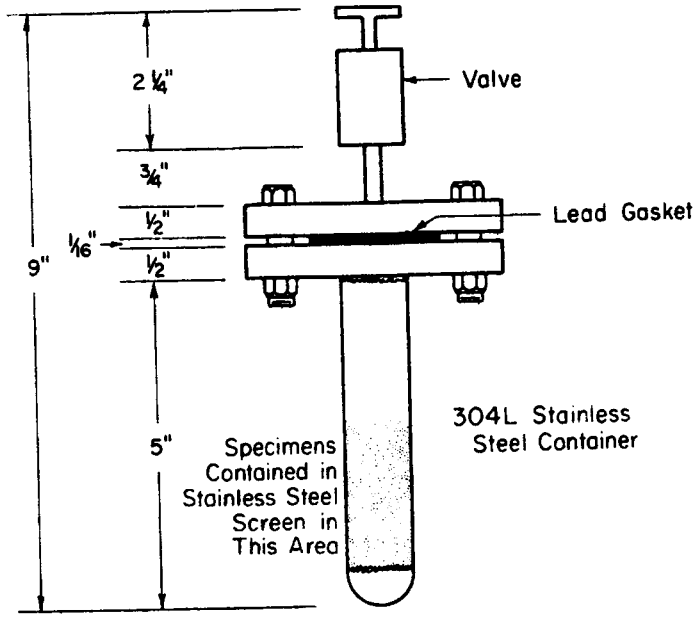

FIG. 1 EXPOSURE CONTAINER FOR SOLUBILITY SPECIMENS

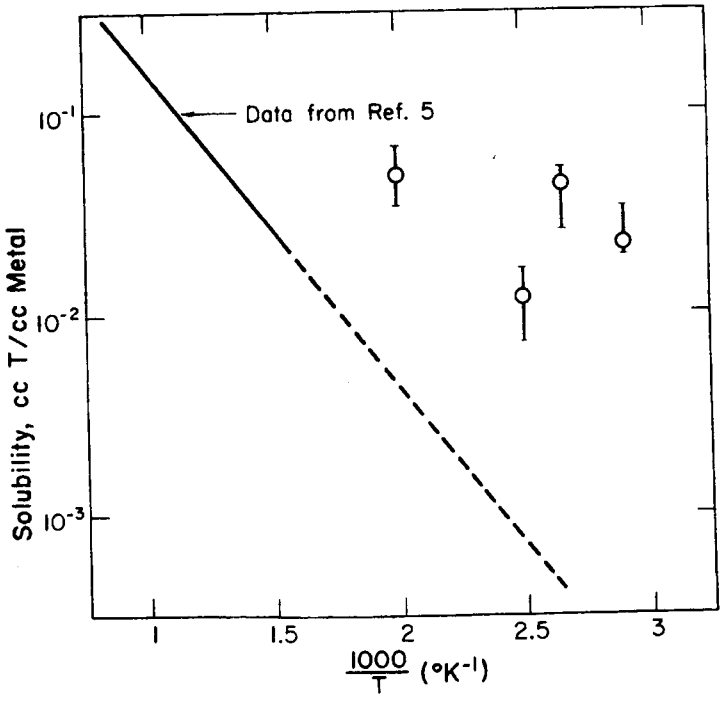

FIG. 2 TRITIUM SOLUBILITY IN IRON - AVERAGE VALUES FOR ALL SPECIMENS

TABLE I

Solubility Specimens

Material	Condition Number	Specimen Condition
MARZ Iron (99.99%)	1	70% cold worked
	2	1 + vacuum annealed at 300°C for 30 hours, furnace cooled
	3	1 + 2 + vacuum annealed at 800°C for 30 hours, furnace cooled
MARZ Nickel (99.995%)	1	70% cold worked
	2	1 + vacuum annealed at 300°C for 30 hours, furnace cooled
	3	1 + 2 + vacuum annealed at 800°C for 50 hours, furnace cooled

The tritium concentrations in the α-Fe specimens were a factor of ten to several hundred higher than expected from extrapolation of high temperature data. Additionally, the temperature dependence of tritium solubility could not be well established because of scatter in the data (Fig. 2); however, for any given exposure temperature the cold-worked specimens had higher tritium concentrations than either annealed sample (except at the highest test temperature, Fig. 3). Average values of the tritium solubility and solubility data extrapolated from high temperatures are shown in Fig. 2. The high tritium concentrations in iron have not been explained; however, it is probable that some form of trapping at structural defects is responsible. The higher concentrations in the cold-worked specimens support the trapping hypothesis.

The average tritium concentrations in high purity nickel, shown in Table II, were in agreement with values extrapolated from data obtained at higher temperatures[5-8] (Fig. 4). As with the iron specimens, the tritium concentration was consistently higher in the cold-worked specimens (Fig. 5). The difference between the cold-worked and the annealed specimens decreased with increasing temperature, as would be expected if the differences were due to tritium segregation to dislocations or other structural defects.

These preliminary solubility studies emphasize the importance of lattice defects in solubility measurements at near-ambient temperatures.

TABLE II

Solubility of Tritium in High Purity Iron and Nickel

		Solubility, $\frac{\text{cc T}}{\text{cc metal}} \times 10^2$			
	Condition[a]	71°C	103°C	127°C	227°C
MARZ Iron	1	1.8	4.06	1.45	6.26
		3.1	4.95	1.07	3.39
	2	2.41	4.90	1.55	5.61
		1.71	3.88	1.23	6.20
	3	1.06	2.39	0.83	3.28
		2.11	4.38	0.67	3.15
		100°C	127°C	227°C	
MARZ Nickel	1	2.76	5.75	10.0	
		2.53	6.47	10.5	
	2	1.68	3.99	8.78	
		1.27	4.81	10.6	
	3	1.53	3.30	8.62	
		1.23	4.30	9.97	

(a) See Table I.

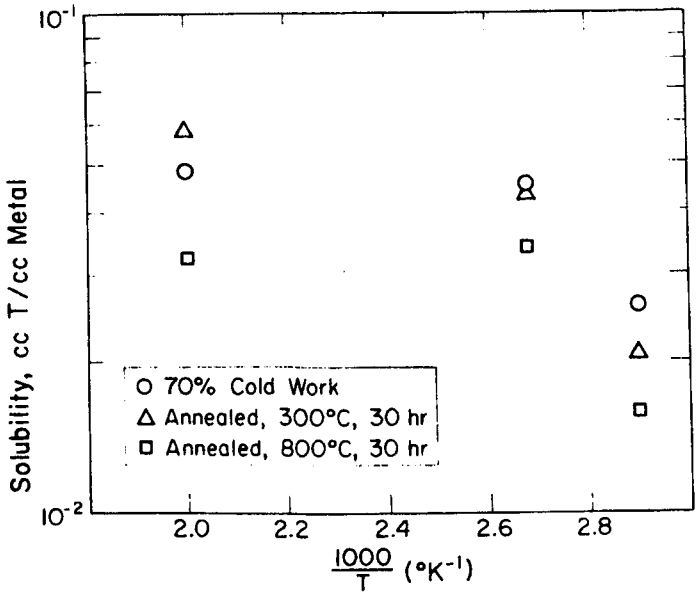

FIG. 3 EFFECT OF SPECIMEN CONDITION AND TEMPERATURE ON TRITIUM SOLUBILITY IN IRON

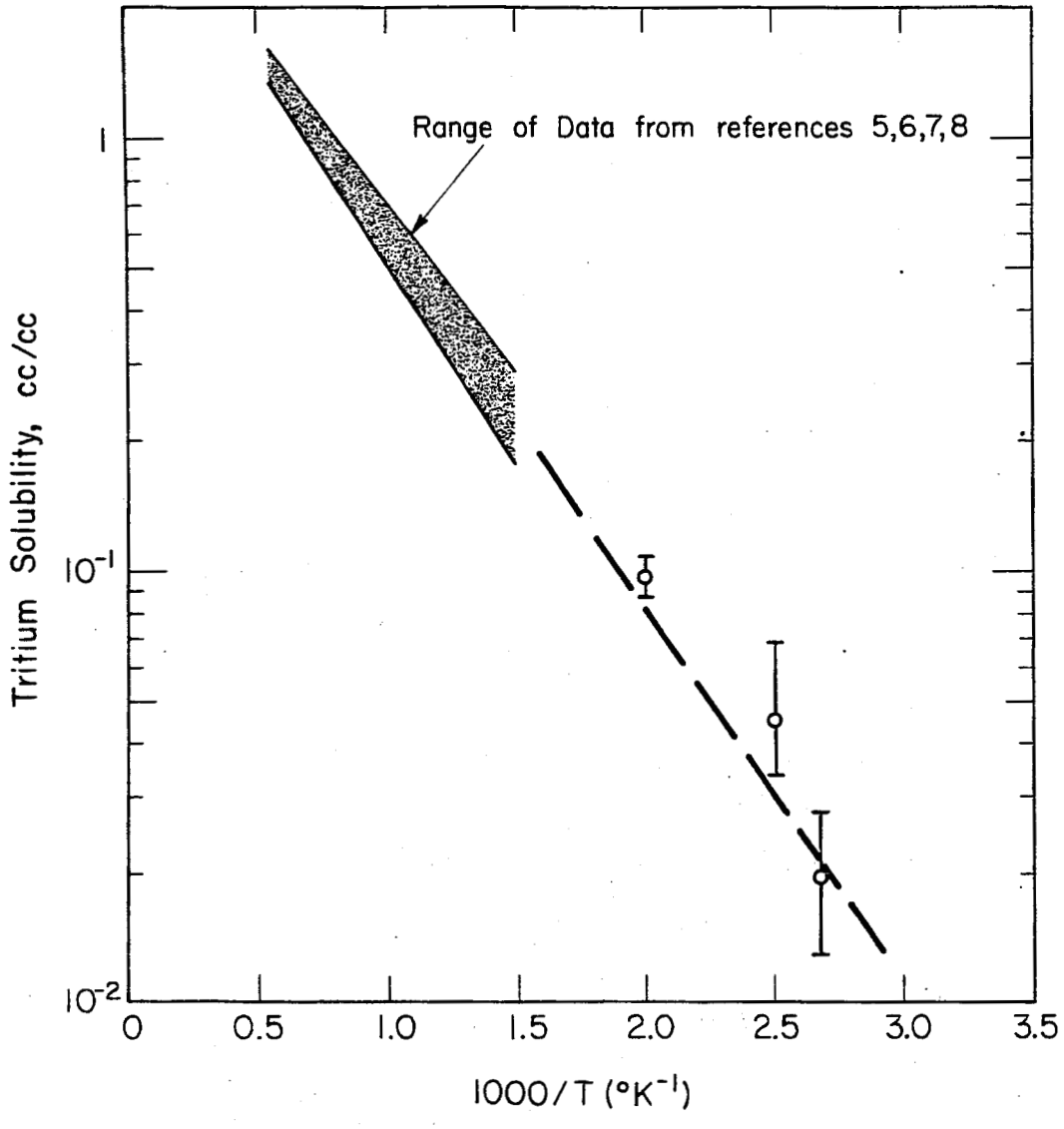

FIG. 4 TRITIUM SOLUBILITY IN NICKEL - AVERAGE VALUES FOR ALL SPECIMENS

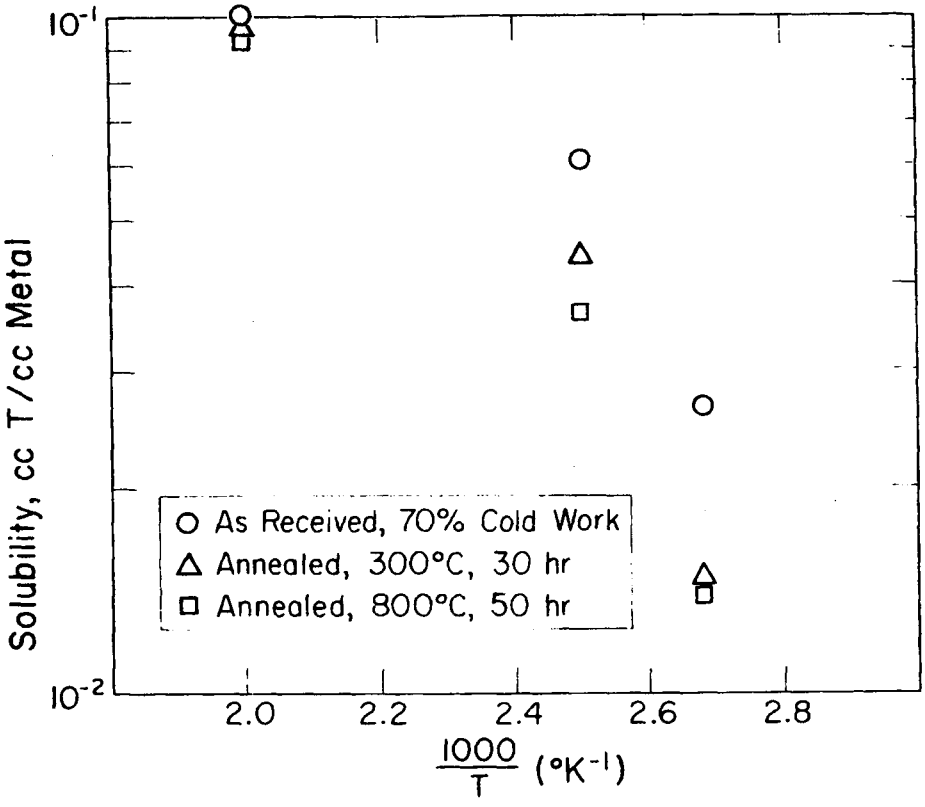

FIG. 5 EFFECT OF SPECIMEN CONDITION AND TEMPERATURE ON TRITIUM SOLUBILITY IN NICKEL

DIFFUSIVITY MEASUREMENTS

The diffusivities of hydrogen in metals near room temperature have been difficult to measure because of lack of sensitivity in measuring apparatus. Cathodic charging experiments may not give true diffusivities because the inherent operating conditions are more severe than those in gas phase experiments.[9] A successful experimental approach to measure hydrogen diffusivity at elevated temperatures measures the outgassing rate as a function of time.[10] Conventional methods for measuring the outgassing rate near room temperature lack the necessary sensitivity, but by using tritium's radioactive properties, the outgassing rate from nickel and iron between room temperature and 200°C can be measured. As described below, the results for nickel are in good agreement with published data. The true value of the diffusivity of hydrogen in iron below about 200°C is uncertain, but preliminary results agree with the lower values of the broad range reported in the literature.

The experimental analysis is based on the solution[11] to Fick's laws for the evolution of a diffusing species from a cylinder of diameter d and length ℓ, which at t = 0 is uniformly saturated with the diffusing species and has an external surface concentration of zero. The total quantity of diffusing species left in the cylinder at time t is given by

$$\frac{Q}{Q_o} = \frac{32}{\pi^2} \sum_{n=1}^{\infty} \frac{1}{\beta_n^2} \exp\left[- \frac{\beta_n^2}{a^2} Dt \right] \sum_{m=0}^{\infty} \frac{1}{(2m-1)^2}$$

$$\exp\left[- \frac{(2m-1)^2 \pi^2 Dt}{\ell^2} \right] \qquad (1)$$

where Q_o is the initial quantity of diffusing species in the specimen, β_n is the n^{th} root of the zero-order Bessel function, a is the radius, and D is the diffusivity. After a short initial time, t_o, the first term of the series becomes dominant, and this expression can be written

$$\frac{Q}{Q_o} = \frac{32}{\pi^2 \beta_1^2} \exp\left[- \left[\frac{\beta_1^2}{a^2} + \frac{\pi^2}{\ell^2} \right] Dt \right] , \text{ for } t > t_o \qquad (2)$$

The rate of evolution of the diffusing species from the specimen, the outgassing rate, is given by

$$- \frac{\partial Q}{\partial t} = \frac{32 Q_o}{\pi^2 \beta_1^2} \left[\frac{\beta_1^2}{a^2} + \frac{\pi^2}{\ell^2} \right] D \exp\left[- \left[\frac{\beta_1^2}{a^2} + \frac{\pi^2}{\ell^2} \right] Dt \right] \qquad (3)$$

The natural logarithm of the outgassing rate is

$$\ln\left[- \frac{\partial Q}{\partial t} \right] = \ln\left[\frac{32 Q_o}{\pi^2 \beta_1^2} \left[\frac{\beta_1^2}{a^2} + \frac{\pi^2}{\ell^2} \right] D \right] - \left[\frac{\beta_1^2}{a^2} + \frac{\pi^2}{\ell^2} \right] Dt \qquad (4)$$

Therefore, a graph of $\ln(-\partial Q/\partial t)$ versus time, after an initial time t_o, is linear with a slope equal to $-(\beta_1^2/a^2 + \pi^2/\ell^2)D$, from which D can be calculated.

The interesting feature of this relationship is that the total quantity of gas in the specimen is not important, because the slope of $\ln(-\partial Q/\partial t)$ versus t is independent of this quantity. Another advantage is that an accurate knowledge of the starting time is not required. The third advantage is that the precise concentration gradient is not needed. These three properties

increase greatly the utility of Equation 4 as a means to determine tritium diffusivity as a function of temperature, since this can be done by simply determining the outgassing rate at one temperature then changing the temperature and repeating the experiment. This process can be repeated until virtually all of the hydrogen or tritium has evolved from the specimen.

Cylindrical specimens were saturated by exposure to 89 mole % tritium gas (the remainder was helium, the radioactive decay product) at 227°C and approximately one atmosphere. After exposure, the specimens were stored until use at -30°C. For the initial experiments, annealed, commercially pure nickel and "Armco" iron were used. The tritium concentration immediately after charging was 5.8×10^{-2} cc T/cc metal for the nickel and 1.44×10^{-1} cc T/cc metal for the "Armco" iron.

The tritium-charged specimens were placed inside a copper chamber (Fig. 6) with a copper-constantan thermocouple attached to the specimen. The copper chamber was immersed in a heated silicone oil bath that was controlled within ±0.5°C. A flow of argon over the specimen carried the tritium released from the specimen to a flowthrough ionization chamber, which measured the quantity of tritium in the gas stream. This quantity is directly proportional to the release rate. By plotting the logarithm of the release rate versus time, and determining the slope of the linear portion of the plot, D was calculated.

The outgassing rate from nickel at 125°C is shown in Fig. 7; zero time was arbitrarily chosen. Fig. 8 shows these same data on a log scale, as well as the results at 89 and 100°C. After some period of time, each graph of $\ln(-\partial Q/\partial t)$ versus t became linear, as predicted by theory. From the slope of the linear portion of the plot, the diffusivity was calculated. These values are given in Table III and plotted in Fig. 9. The diffusivity of hydrogen was determined by multiplying the measured tritium diffusivity by $\sqrt{3}$ to account for the mass effect. The dashed lines in Fig. 9 represent the spread in diffusivity data in the published literature. Table IV (taken from Reference 12) lists the experimental method, the temperature, D_o, and the activation energy determined by other investigators for hydrogen diffusion in nickel. The present investigations show that the diffusivity of tritium in nickel can be expressed as

$$D = 1.7 \times 10^{-3} \exp(-8600/RT) \text{ cm}^2 \text{ sec}^{-1} \quad (5)$$

which is in good agreement with other investigations.

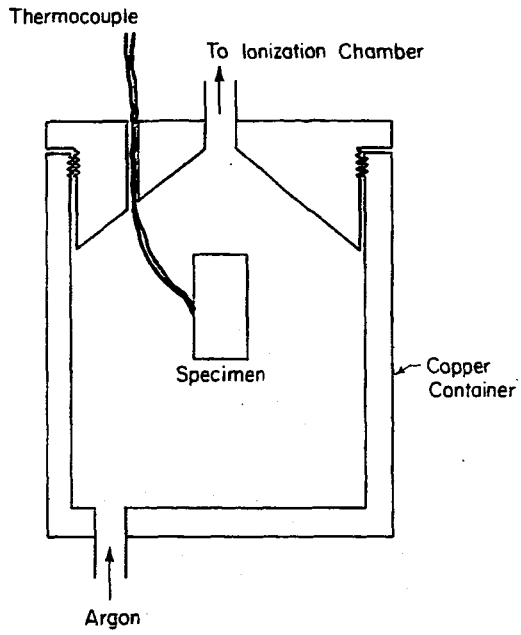

FIG. 6 CHAMBER USED TO CONTAIN TRITIATED SPECIMENS FOR OUTGASSING RATE MEASUREMENTS

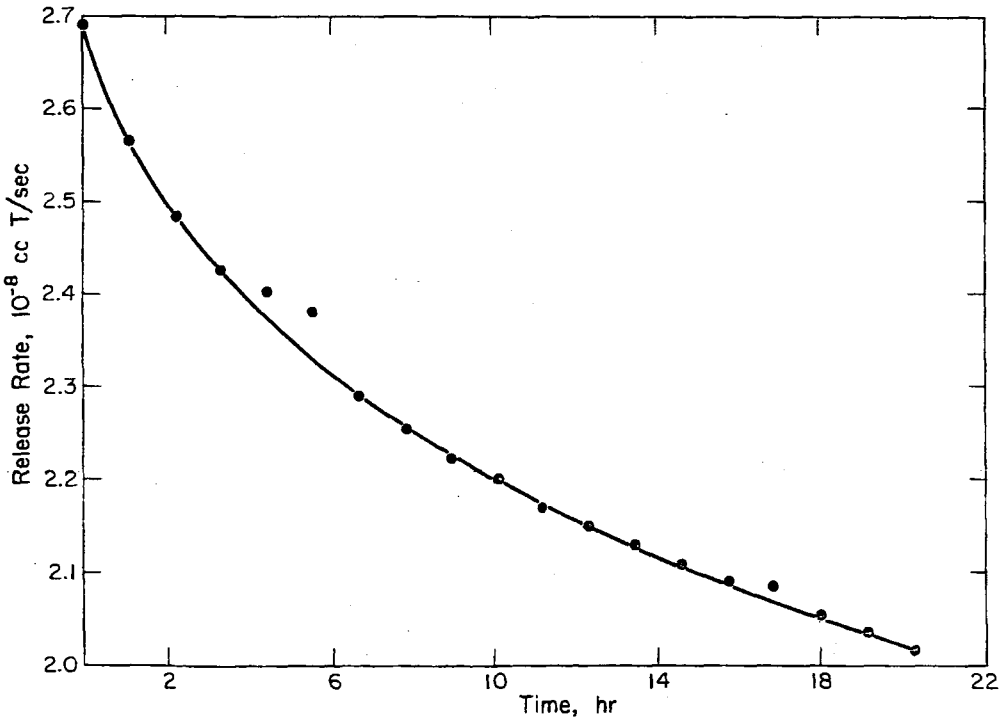

FIG. 7 TRITIUM RELEASE RATE FROM NICKEL AS A FUNCTION OF TIME AT 125°C

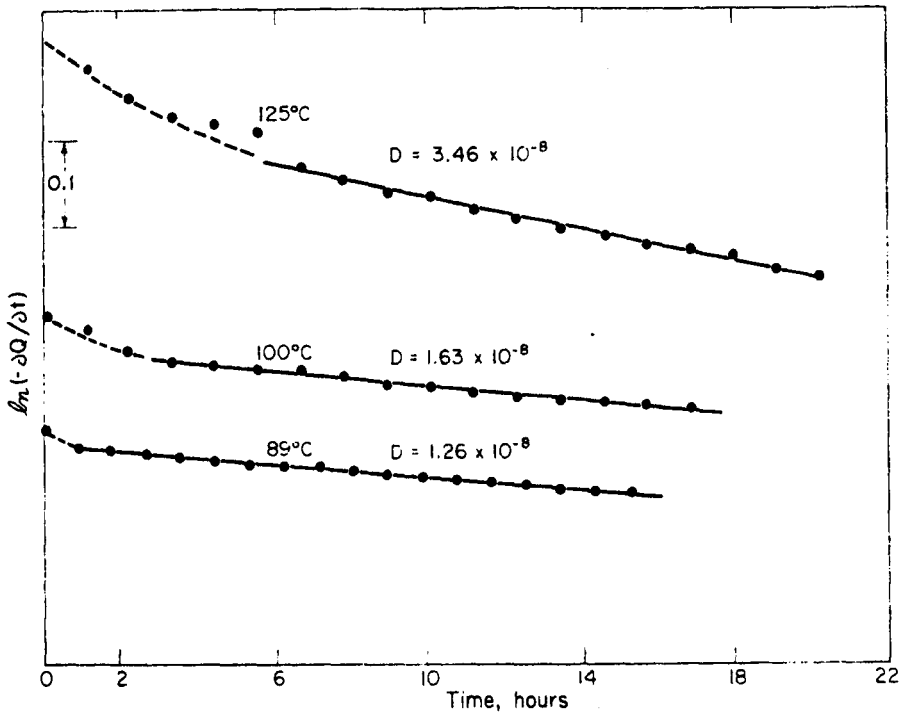

FIG. 8 TRITIUM RELEASE RATE FROM NICKEL AS A FUNCTION OF TIME

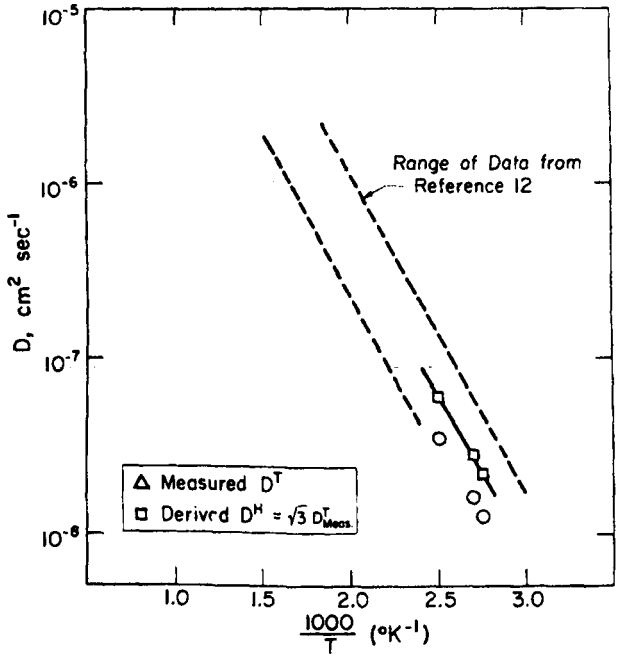

FIG. 9 TEMPERATURE DEPENDENCE OF TRITIUM DIFFUSIVITY IN NICKEL

TABLE III

Diffusivity of Tritium in Nickel

Temperature, °C	Diffusivity, $cm^2\ sec^{-1}$
89	1.26×10^{-8}
100	1.63×10^{-8}
125	3.46×10^{-8}

TABLE IV

Representative Diffusivities of Hydrogen in Nickel

$D = D_0 \exp(-E/RT)$

Method of Determination	Temperature Range, °C	D_0, $cm^2\ sec^{-1}$	Activation Energy (E), $cal\ mole^{-1}$
From Reference 12			
Permeation	200-550	0.017	10,800
Permeation	478-798	0.0011	8,400
Permeation	376-600	0.015	10,600
Evolution	85-165	0.00204	8,700
Permeation	248-400	0.023	10,800
Absorption[a]	400-600	0.001	5,500
Evolution	380-986	0.00447	8,600
Evolution	400-700	0.0076	9,880
Evolution	162-496	0.0107	10,125
Permeation	430-850	0.0095	10,300
Evolution	303-694	0.00422	8,400
SRL Results			
Evolution	89-125	0.0017	8,600

(a) Not shown in Fig. 9.

The diffusivity of tritium in "Armco" iron was determined between 38 and 200°C. Fig. 10 shows the natural logarithm of the release rate as a function of time at 125 and 150°C for one specimen, and at 200°C for another specimen. The 125 and 150°C curves show a discontinuity, which was also present for outgassing at 100 and 200°C for this specimen only. The explanation for this discontinuity is not known. Values for the diffusivity of tritium in iron are listed in Table V.

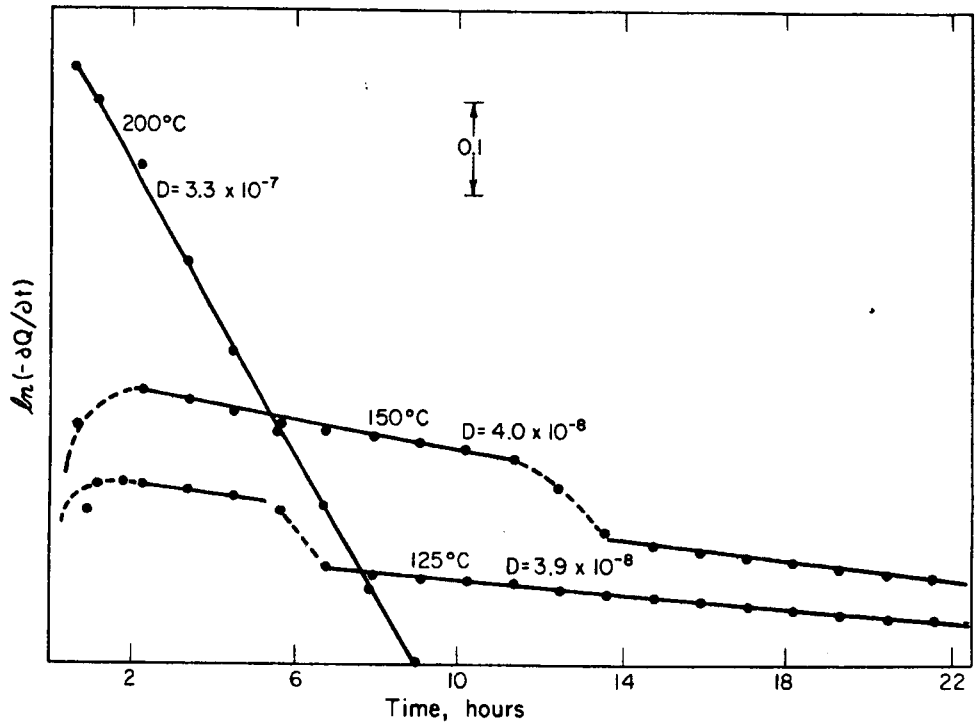

FIG. 10 TRITIUM RELEASE RATE FROM IRON AS A FUNCTION OF TIME

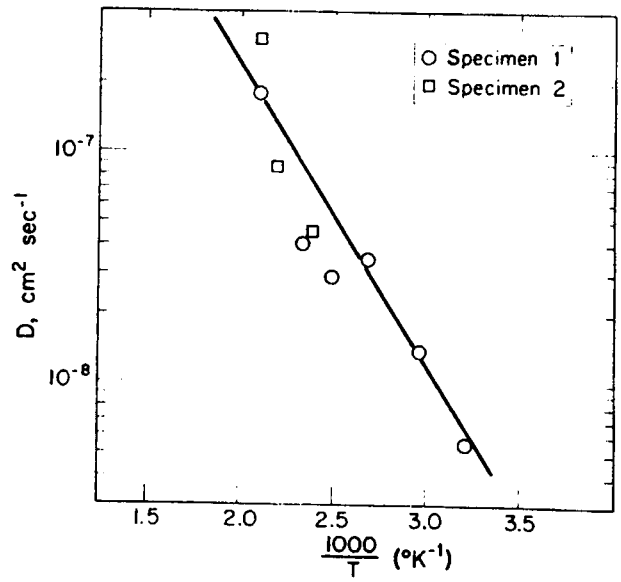

FIG. 11 TEMPERATURE DEPENDENCE OF TRITIUM DIFFUSIVITY IN IRON

TABLE V

Diffusivity of Tritium in Iron

Specimen Number	Temperature, °C	Diffusivity, $cm^2\ sec^{-1}$
1	28	5.6×10^{-9}
	64	1.3×10^{-8}
	100	3.6×10^{-8}
	125	3.9×10^{-8}
	150	4.0×10^{-8}
	200	1.8×10^{-7}
2	138	4.5×10^{-8}
	180	8.5×10^{-8}
	200	3.3×10^{-7}

The temperature dependence of tritium diffusivity in iron is shown in Fig. 11; these values after adjustment for the mass effect are compared with the previous data[9] in Fig. 12. The equation representing hydrogen diffusion as a function of temperature is

$$D = 1.2 \times 10^{-4} \exp(-6140/RT),\ cm^2/sec$$

As shown in Fig. 12, these experimental values are at the low end of the range of the broad band of values previously reported for hydrogen diffusion in iron.

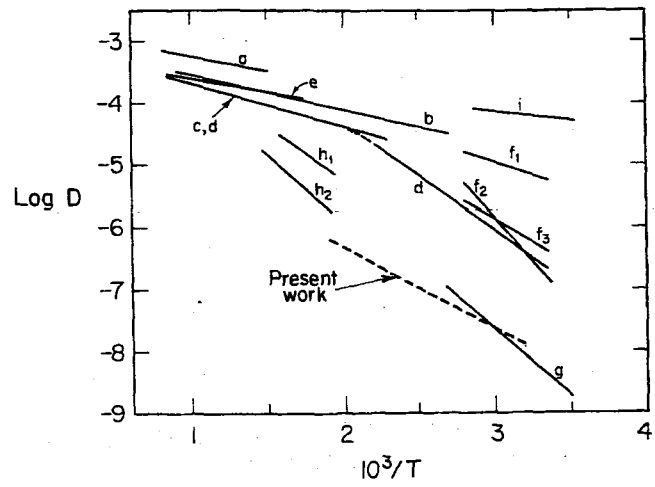

FIG. 12 REPRESENTATIVE DATA FOR DIFFUSIVITY OF HYDROGEN IN IRON (Letters on Lines Refer to References in Ref. 9)

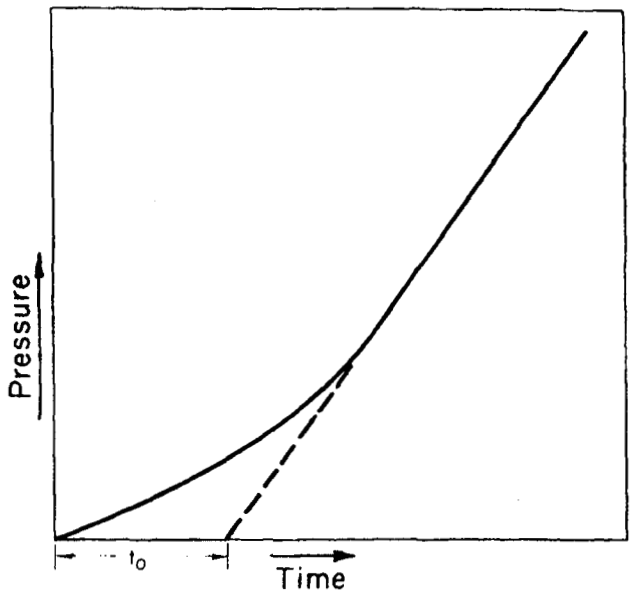

FIG. 13 CHARACTERISTIC PERMEATION CURVE USED FOR TIME-LAG ANALYSIS

PERMEATION MEASUREMENTS

Hydrogen permeation through a membrane has been frequently measured to determine the permeability and diffusivity of hydrogen in metals. The total amount of hydrogen, Q, which passes through a membrane of area A, and thickness τ, under the boundary conditions that $C = C_1$ at $X = 0$ and $C = 0$ at $X = \tau$, is given by the equation[13]

$$Q = A\tau C_1 \left[\frac{Dt}{\tau^2} - \frac{1}{6}\right] - \frac{2A}{\pi^2} \sum_{n=1} \frac{1}{(-n^2)} n \exp - \left[\frac{Dn^2\pi^2 t}{\tau^2}\right] \qquad (7)$$

$$\text{As } t \to \infty,\ Q = \frac{ADC_1}{\tau} \left[t - \frac{\tau^2}{6D}\right] \qquad (7a)$$

Therefore, the intercept of the extrapolated permeation curve on the time axis is $t_o = \tau^2/6D$ (Fig. 13). This type of analysis can be used to obtain D and is known as the "time-lag" analysis.

The permeability, ϕ, is defined by the equation[4]

$$Q = \phi t \frac{A}{\tau} (P_i^{\frac{1}{2}} - P_o^{\frac{1}{2}}) \qquad (8)$$

where A is the area through which the gas is permeating, and P_i and P_o are the pressure on the input and output sides, respectively. The units of permeability, ϕ, are cm^3 (NTP H_2) cm^{-1} sec^{-1} $atm^{-\frac{1}{2}}$. P_o for the usual permeation test is very near zero on the output side, therefore satisfying the boundary conditions used for the time-lag analysis.

The permeation system required for these studies was fabricated and tested initially with T-1 steel and with high purity iron. The T-1 steel was in the as-received condition, and was 0.035-inch thick. Two high purity iron specimens were tested: one was cold worked 92% to 0.040 inch, and another was cold worked 99% in thickness to 0.005 inch and then annealed 1/2 hour at 750°C

A schematic diagram of the permeation system is shown in Fig. 14. The specimen was bolted between the two stainless steel blocks and sealed with lead gaskets. The system was evacuated to approximately 10^{-5} torr. A cold trap between the diffusion pump and the system reduced oil backstreaming into the permeation system. The permeation system was operated as follows: Cylinder hydrogen gas, purified by passing it through a palladium-silver diffuser, entered the system through line a into line b (valves B, C, D, and E closed) until 90 psi hydrogen was obtained. Then valves H and G were closed and valve C was opened. This admitted hydrogen to the input side of the specimen and caused the pressure to drop to 85 psi. Additional hydrogen was added until the pressure built up to 90 psi; then valve C was closed and valve F was opened for the duration of the test. As soon as the hydrogen was admitted to the specimen, the pressure on the output side was measured as a function of time with a capacitance-type gage, which indicates changes in pressure directly and is independent of the properties of the particular gas. Two different measuring heads were used, one with a range of 1 to 1000 mm and another with a range of 0.01 to 10 mm. The output from the gage was continuously recorded during the test.

Prior to each test the leak rate of the system was determined and the permeation measurements were corrected to allow for such leakage, although in no case was the inleakage significant when compared to the hydrogen pressure buildup.

The specimen was heated in a clam shell furnace. The temperature was measured by two thermocouples, one adjacent to each side of the specimen embedded in the stainless steel blocks. The temperature control during a test was ±1.0°C.

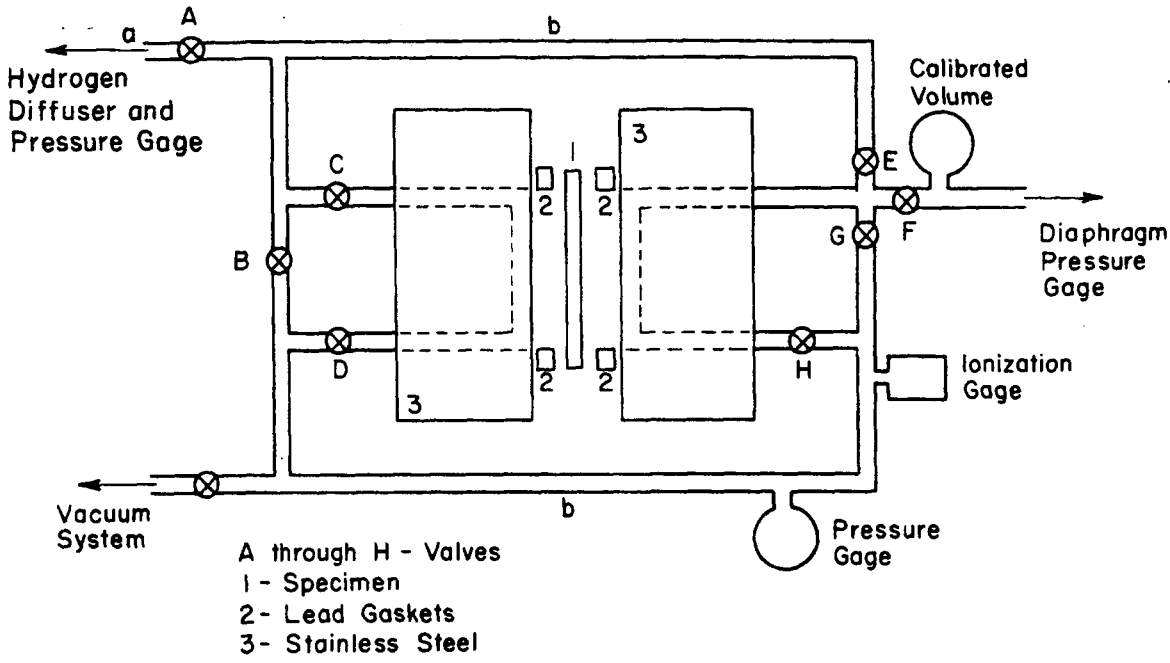

FIG. 14 SCHEMATIC REPRESENTATION OF PERMEATION SYSTEM

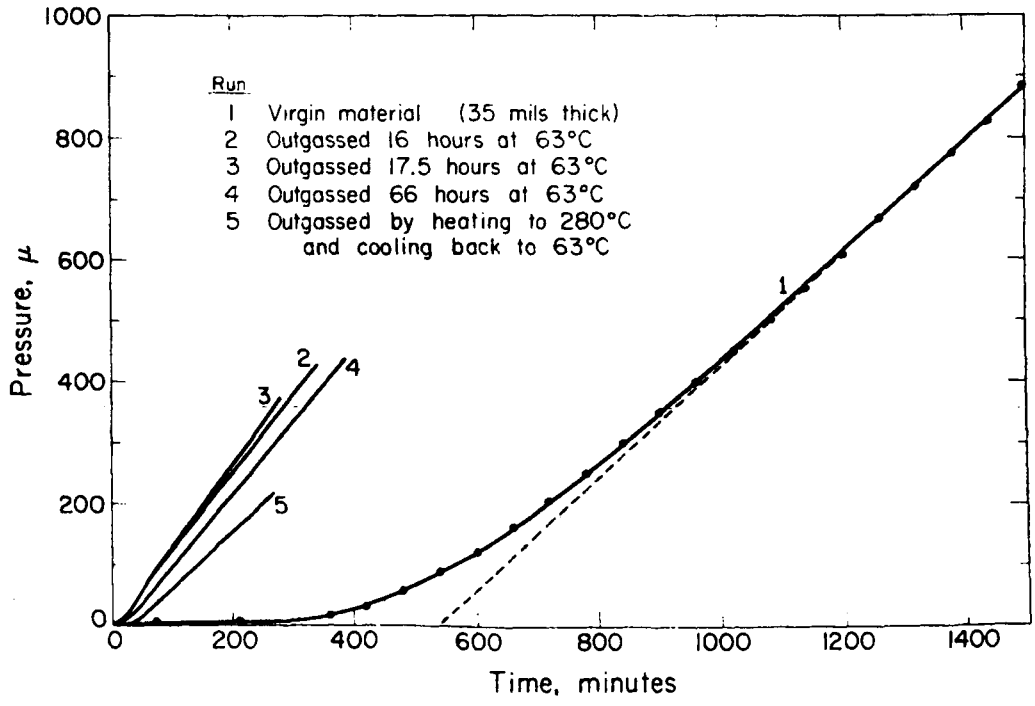

FIG. 15 PERMEATION OF HYDROGEN THROUGH T-1 STEEL

The permeability of hydrogen through the T-1 steel was measured in the temperature range 60 to 150°C. Fig. 15 is a plot of the pressure of hydrogen on the output side for the initial permeation test on a given specimen, and subsequent tests on the same specimen after several different outgassing treatments. The permeability is determined from the slope of the linear portion of the curve. The results at 66 and 94°C were similar, and values for permeability, ϕ, are listed in Table VI.

TABLE VI

Permeability and Diffusivity of Hydrogen in T-1 Steel

Specimen Number	Run Number	Temperature, °C	ϕ, $cm^3\ cm^{-1}\ sec^{-1}\ atm^{-\frac{1}{2}}$	D, $cm^2\ sec^{-1}$
1	1	60	4.8×10^{-9}	4.1×10^{-8}
1	2	63	7.2×10^{-9}	1.7×10^{-6}
1	3	63	7.4×10^{-9}	1.7×10^{-6}
1	4	63	6.7×10^{-9}	9.5×10^{-7}
1	5	63	5.1×10^{-9}	5.5×10^{-7}
1	6	96	2.3×10^{-8}	2.0×10^{-6}
1	7	116	3.9×10^{-8}	4.4×10^{-6}
1	8	149	1.05×10^{-7}	1.45×10^{-5}
2	1	66	8.2×10^{-9}	2.6×10^{-7}
2	2	66	8.7×10^{-9}	1.7×10^{-6}
3	1	94	2.45×10^{-8}	4.2×10^{-7}
3	2	94	2.0×10^{-8}	3.0×10^{-6}

Outgassing the specimen before test had little effect on the steady-state permeability. (This was not true for the apparent diffusivity determined by time-lag analysis, see below.) Hydrogen permeability as a function of temperature is shown in Fig. 16 and can be expressed by the equation

$$\phi = 5.7 \times 10^{-3} \left[\exp(-9100/RT)\right] \frac{cm^3}{cm\ sec\ atm^{\frac{1}{2}}} \qquad (10)$$

which is in fair agreement with the equation derived by Gonzalez[4] from a critical analysis of the literature.

Diffusivity, as determined by the time-lag analysis, was much lower on the initial permeation test than on subsequent runs on the same specimen, even though the specimen was outgassed before each run. This phenomenon has been reported by other investigators.[14] At 60°C, the first test gave $D = 4.1 \times 10^{-8}$ $cm^2\ sec^{-1}$, but subsequent runs after various outgassing treatments gave D's between 0.55 and 1.7×10^{-6} $cm^2\ sec^{-1}$, a factor of 13 to 40 higher than the initial run. Results at 66 and 94°C were qualitatively the same as those for 60°C, and values determined are given in Table VI.

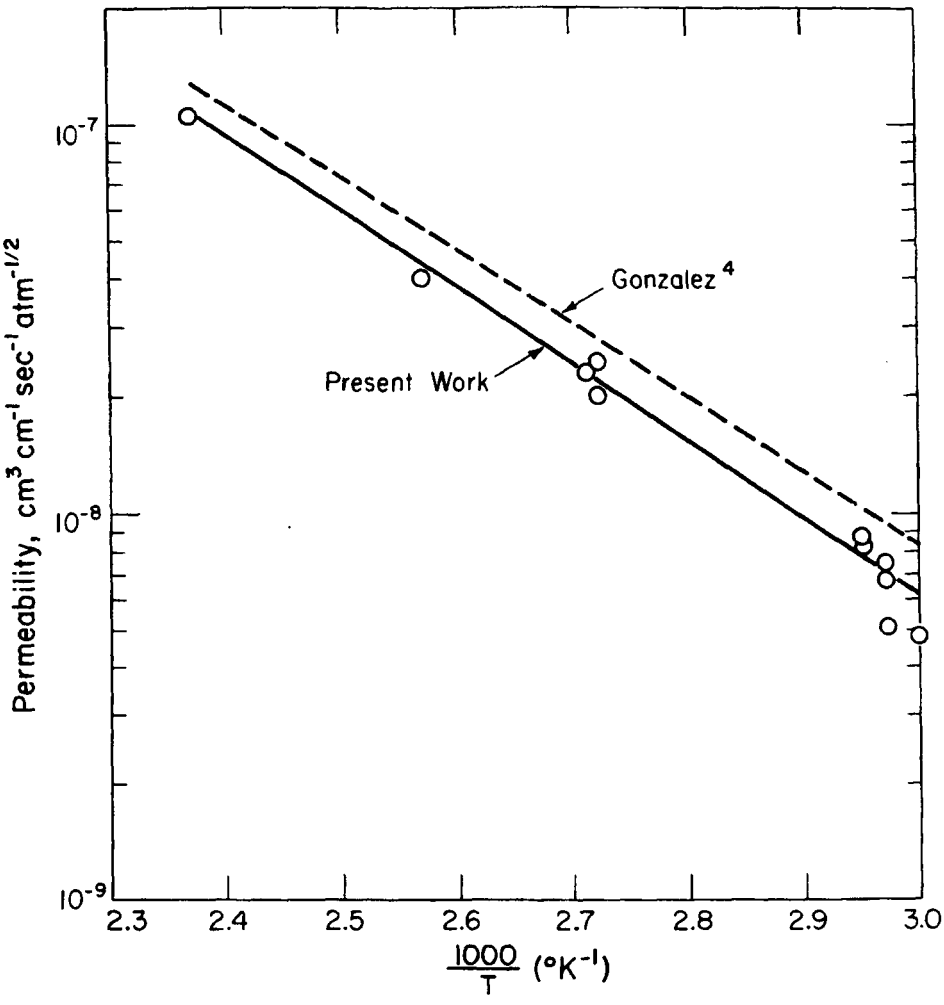

FIG. 16 TEMPERATURE DEPENDENCE OF HYDROGEN PERMEABILITY IN T-1 STEEL

One of the necessary boundary conditions for use of the time-lag analysis is that the specimen be initially free of hydrogen. It is likely that the outgassing treatments did not remove all of the hydrogen from the specimen; therefore, the application of the time-lag analysis may not be valid, except for the initial tests.

The diffusivity calculated from the initial test is also questionable because of immobilization of hydrogen by trapping[9,15] at various lattice defects. Until steady-state permeation is achieved, some of the hydrogen entering the specimen may be diverted from the simple permeation process into lattice traps; therefore, even the diffusivity calculated from the initial permeation test may not be the true diffusivity. The only property unambiguously determined by the permeation measurements is the permeability which is obtained at steady-state conditions. The diffusivities derived from permeation type tests at best represent "apparent diffusivities", and do not necessarily represent the true diffusivity of hydrogen through a defect-free lattice.

The permeation tests on the high purity iron gave results qualitatively similar to the tests on T-1 steel. Fig. 17 shows the permeation curves for the 0.040-inch-thick, 92% cold-worked specimen. Fig. 18 is for the 0.005-inch-thick, annealed specimen. The values for the permeability and diffusivity are given in Table VII.

TABLE VII

Permeability and Diffusivity of Hydrogen in High Purity Iron

Material Condition	Run No.	Temp, °K	ϕ, $cm^3\ cm^{-1}\ sec^{-1}\ atm^{-\frac{1}{2}}$	D, $cm^2\ sec^{-1}$
Annealed	1	298	0.4×10^{-10}	3.7×10^{-10}
(0.005-inch-thick)	2	298	1×10^{-9}	4.1×10^{-9}
92% Cold Worked	1	298	1.02×10^{-9}	7.65×10^{-9}
(0.040-inch-thick)	2	298	1.64×10^{-9}	8.2×10^{-7}
	3	298	1.7×10^{-9}	1.6×10^{-7}
	4	298	1.5×10^{-9}	1.3×10^{-7}
	5	298	1.3×10^{-9}	1.1×10^{-7}

The "diffusivities" in the cold-worked high purity iron specimens were less than those obtained for the annealed specimen. This may be the effect of deformation on diffusivity or an effect of specimen size, as observed by other investigators.[15] The diffusivities calculated for the initial and second runs differed by a factor of 10 in the annealed material and by a factor of 100 in the cold-worked material. This variation may be a result of the influence of the higher density of traps in the deformed material.

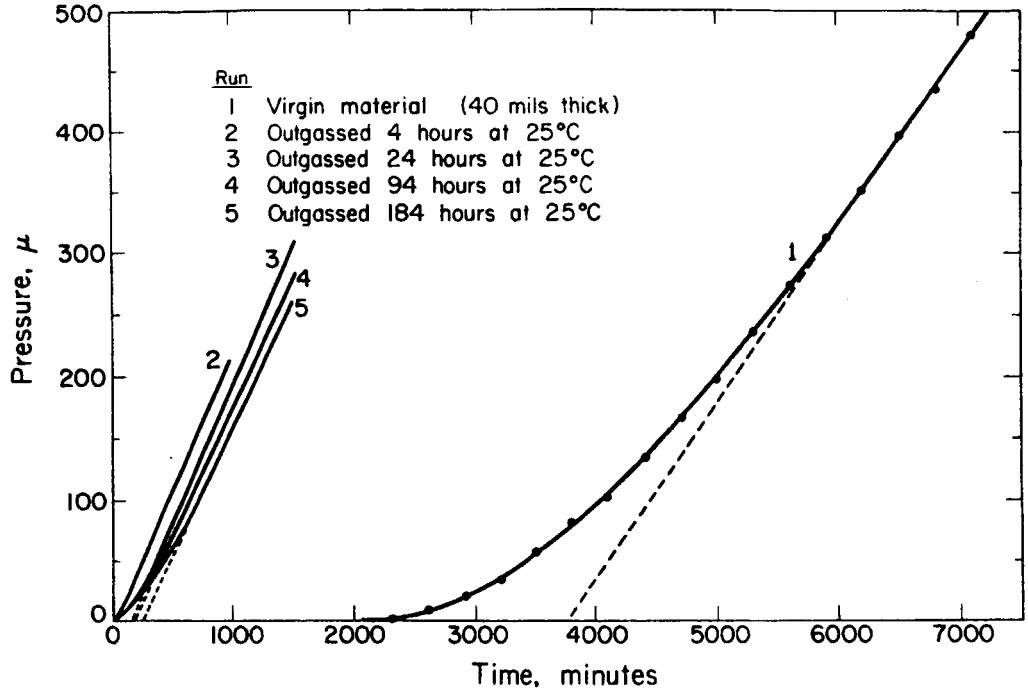

FIG. 17 PERMEATION OF HYDROGEN THROUGH 92% COLD-WORKED IRON

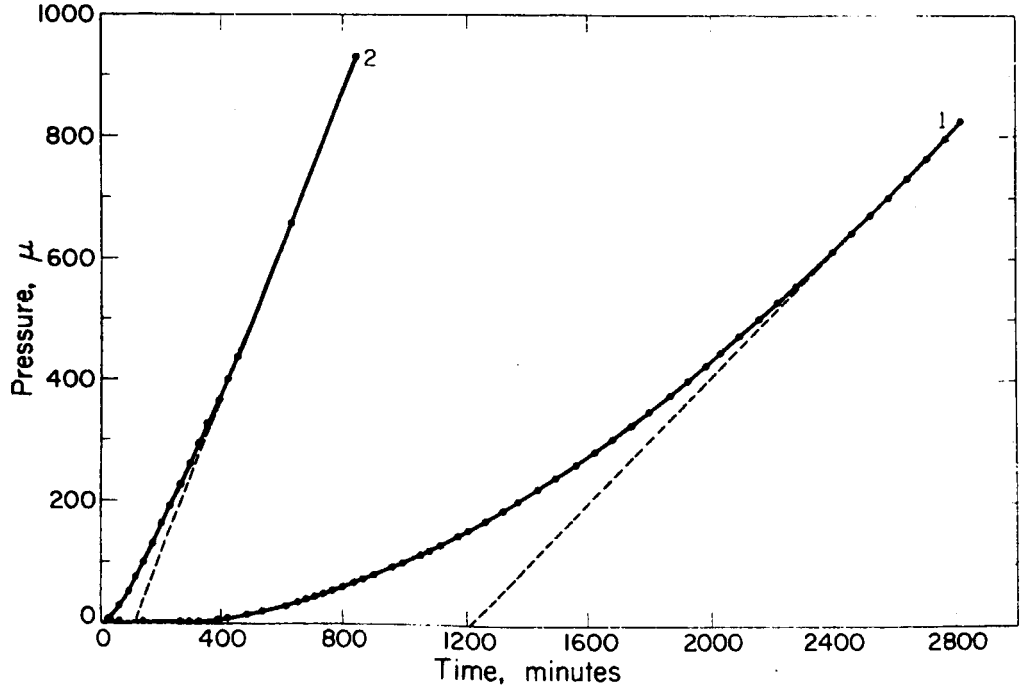

FIG. 18 PERMEATION OF HYDROGEN THROUGH ANNEALED IRON (Specimen 5 mils thick, test at 25°C)

ELECTRON MICROSCOPY

A principal objective of the program is to correlate the microstructure of the specimens with their solubility, diffusivity, and permeability. Electron microscopy is being used to characterize the substructure of the specimens after various amounts of deformation and various annealing treatments. At this time the electron microscopy and property measurements are not complete enough to allow even a preliminary correlation. The results will be reported at a later date.

PROGRAM

It is planned to continue solubility, diffusivity, and permeability measurements on high purity iron and nickel, and to extend the studies to the commercial T-1 and A-350 steels in future testing. The interrelation of solubility, diffusivity, and permeability will be studied by independent determination of each property. The properties will also be studied as a function of the deformation and grain size because it is thought that the damage caused by hydrogen in metals is due to its interactions with such structural imperfections. The microstructure of the specimen, when pertinent, will be characterized by electron microscopy. The analysis of trapping developed by McNabb and Foster[16] will be used as a guide to design experiments and will be applied to the data when possible.

The measurements on the high purity materials will have priority over the commercial steels because results obtained on such specimens should be easier to interpret, and will serve as a basis to understanding the effect of hydrogen in the more complex commercial steels.

REFERENCES

1. Brown Engineering Company Report No. 415. NAS-10-1360. October 1966.

2. R. L. Mills and F. J. Edeskuty. "Tests for Hydrogen Embrittlement of Steels Used in Tank Farm Cylinders." LA-3602-MS. Los Alamos Scientific Laboratory. November 1966.

3. "Effects of High Pressure Hydrogen on Storage Vessel Materials." Rocketdyne Report R-6851. NAS-8-19. January 1967.

4. O. D. Gonzalez. "The Measurement of Hydrogen Permeation in Alpha Iron: An Analysis of the Experiments." *Trans. AIME 245*, 607 (1969).

5. A. Sieverts. As reported in *Scientific Foundations of Vacuum Techniques*. S. Dushman, 2nd Ed., p 525. J. Wiley & Sons, Inc., New York (1962).

6. J. Smittenberg. As reported in *Scientific Foundations of Vacuum Techniques*. S. Dushman, 2nd Ed., p 525. J. Wiley & Sons, Inc., New York (1962).

7. M. H. Armbruster. As reported in *Scientific Foundations of Vacuum Techniques*. S. Dushman, 2nd Ed., p 525. J. Wiley & Sons, Inc., New York (1962).

8. L. Luckemeyer-Hasse and H. Schenck. As reported in *Scientific Foundations of Vacuum Techniques*. S. Dushman, 2nd Ed., p 525. J. Wiley & Sons, Inc., New York (1962).

9. R. A. Oriani. "Hydrogen in Metals." *Fundamental Aspects of Stress Corrosion Cracking, Ohio State University, 1967.* Nat'l. Assoc. of Cor. Eng., 32, 1969.

10. M. L. Hill and E. W. Johnson. "Diffusivity of Hydrogen in Nickel." *Acta Met. 3*, 566 (1955).

11. A. Demarez, A. G. Hock, and F. A. Meunier. "Diffusion of Hydrogen in Mild Steel." *Acta Met. 2*, 214 (1954).

12. T. Boniszewski and G. C. Smith. "The Influence of Hydrogen on the Plastic Deformation, Ductility, and Fracture of Nickel in Tension." *Acta Met. 11*, 165 (1963).

13. J. Crank. *The Mathematics of Diffusion, 1st Ed., p. 47.* Oxford University Press, London (1956).

14. M. A. V. Devanathan, Z. Stachurski, and W. Beck. "A Technique for Evaluation of Hydrogen Embrittlement Characteristics of Electroplating Baths." *J. Electrochem. Soc. 110*, 886 (1963).

15. W. Roczynski and M. Smialowski. *Hydrogen in Steel, p. 71.* Pergamon Press Ltd., U.S.A. Ed. Addison-Wesley Pub. Co., Reading, Mass. (1962).

16. A. McNabb and P. K. Foster. "A New Analysis of the Diffusion of Hydrogen in Iron and Ferritic Steels." *Trans. AIME 227*, 618 (1963).

APPENDIX

CHEMICAL COMPOSITION OF MATERIALS USED

A. MARZ Grade Iron

(Vendor: Materials Research Corporation)

Element	Content, ppm	Element	Content, ppm
Li	0.004	Rh	<0.03
Be	0.005	Pd	<0.08
B	<0.0008	Ag	<0.04
C	25.0	Cd	<0.08
N_2	7.0	In	<0.06
O_2	25.0	Sn	<0.02
H_2	<0.1	Sb	<0.02
F	Interference	Te	<0.07
Na	0.8	I	<0.007
Mg	8.0	Cs	<0.006
Al	Interference	Ba	0.04
Si	<0.5	La	<0.006
P	0.3	Ce	<0.006
S	1.2	Pr	<0.006
Cl	3.0	Nd	<0.02
K	0.2	Sm	<0.025
Ca	2.0	Eu	<0.012
Sc	<0.025	Gd	<0.025
Ti	0.5	Tb	<0.006
V	<0.1	Dy	<0.03
Cr	0.6	Ho	<0.01
Mn	<0.1	Er	<0.4
Fe	-	Tm	<0.3
Co	0.3	Yb	<0.02
Ni	1.2	Lu	<0.006
Cu	<0.2	Hf	<0.025
Zn	<0.8	Ta	<1.0
Ga	<0.5	Re	<0.012
Ge	<1.0	Os	<0.02
As	<0.1	Ir	<0.012
Se	<1.0	Pt	<0.025
Br	<0.15	Au	0.4
Rb	<0.08	Hg	<0.03
Sr	<0.08	Tl	<0.012
Y	<0.04	Pb	<0.015
Zr	<0.06	Bi	<0.008
Nb	0.03	Th	<0.008
Mo	0.2	U	<0.008
Ru	<0.1		

B. MARZ Grade Nickel

(Vendor: Materials Research Corporation)

Impurity	Content, ppm	Impurity	Content, ppm
C	17	Mo	0.5
H	0.2	Na	0.04
O	18	Nb	<0.02
N	3	Pb	<0.02
Ag	<0.02	Pd	<0.03
Al	0.3	Pt	<0.03
Bi	<0.01	Rh	<0.01
Ca	0.1	S	<0.12
Cd	<0.08	Si	0.2
Co	<0.1	Sn	<4
Cr	1.5	Ta	<0.5
Cu	<0.04	Ti	0.15
Fe	12	V	<0.01
K	0.2	W	1.5
Hf	<0.03	Zn	<0.4
Mg	0.02	Zr	<0.15
Mn	0.03		

C. T-1 Steel

(Vendor: U. S. Steel)

Element	Content, %
C	0.1 - 0.2
Mn	0.6 - 1.0
P	0.04
S	0.04
Si	0.15 - 0.35
Ni	0.7 - 1.0
V	0.03 - 0.08
Mo	0.4 - 0.6
Cr	0.4 - 0.65
Cu	0.15 - 0.5
B	0.002 - 0.006

D. "Armco" Iron

(Vendor: Armco Steel Co.)

Element	Content, wt %
C	0.012
Mn	0.017
P	0.005
S	0.025

E. Nickel 270

(Vendor: International Nickel Co.)

Element	Content, wt %
Ni	99.98
C	.01
Mn	<.001
Fe	.001
Cu	<.001
Cr	<.001
S	<.001
Si	.001
Mg	<.001
Ti	<.001
Co	<.001

DISTRIBUTION

1-3	AEC, SROO
4-67	Du Pont Company, Atomic Energy Division
68-69	Rensselaer Polytechnic Institute
70	Rocketdyne Division, North American Rockwell Corp.
71-73	Battelle Memorial Institute
74	McDonnell-Douglas Corporation
75	Astronuclear Laboratory, Westinghouse
76	U. S. Steel Research Laboratory
77	Boeing Co.
78-79	NASA Lewis Research Center
80	NASA Marshall Space Flight Center
81-82	NASA J. F. Kennedy Space Center
83-84	NASA Manned Spacecraft Center
85	NASA Ames Research Center
86	NASA Langley Research Center